On the Study of Resonance Interactions and Splittings in the PH$_3$ Molecule: ν_1, ν_3, $\nu_2 + \nu_4$, and $2\nu_4$ Bands

O. N. Ulenikov,* E. S. Bekhtereva,* V. A. Kozinskaia,* Jing-Jing Zheng,† Sheng-Gui He,† Shui-Ming Hu,†
Qing-Shi Zhu,† C. Leroy,‡ and L. Pluchart‡

*Laboratory of Molecular Spectroscopy, Physics Department, Tomsk State University, Tomsk, 634050, Russia, and Institute of Atmospheric Optics SB RAN,
Tomsk, 634055, Russia; †Open Laboratory of Bond Selective Chemistry, University of Science and Technology of China, Hefei, 230026, China;
and ‡Laboratoire de physique, UMR CNRS 5027, Université de Bourgogne, 9 Avenue A. Savary, B.P. 47 870, F-21078 Dijon, France

E-mail: Ulenikov@phys.tsu.ru; smhu@ustc.edu.cn

The high-resolution (0.005 cm^{-1}) Fourier transform infrared spectrum of PH$_3$ is recorded and analyzed in the region of the fundamental stretching bands, ν_1 and ν_3. The $\nu_2 + \nu_4$ and $2\nu_4$ bands are taken into account also. Experimental transitions are assigned to the ν_1, ν_3, $\nu_2 + \nu_4$, and $2\nu_4$ bands with the maximum value of quantum number J equal to 15, 15, 13, and 15, respectively. a_1–a_2 splittings are observed and described up to the value of quantum number K equal to 10. The analysis of a_1/a_2 splittings is fulfilled with a Hamiltonian model which takes into account numerous resonance interactions among all the upper vibrational states.   © 2002 Elsevier Science (USA)

1. INTRODUCTION

The PH$_3$ molecule is the object of a large spectroscopic interest for a lot of reasons. On the one hand, study of the phosphine spectra is important for some astrophysical applied problems because phosphine was found in the atmospheres of the giant planets Saturn and Jupiter (*1–5*). On the other hand, the PH$_3$ molecule is of interest from a purely theoretical point of view because it is one of the lightest pyramidal molecules. As a consequence, numerous spectroscopic effects and peculiarities which are inherent in such molecules should be particularly pronounced in the spectra of phosphine. An additional interest in the spectroscopic study of the PH$_3$ molecule is caused by the fact that the PH$_3$ molecule can probably be considered as one of the lightest local mode molecules.[1] So both the local mode properties and the conditions of their destruction can be analyzed in the stretching bands of the phosphine molecule. To discuss and solve both the above-mentioned and other problems, first of all, correct assignments of transitions and description of possible peculiarities in experimental spectra should be fulfilled. Accurate experimental information can also be considered an important addition to modern databases.

Earlier, the spectra of the PH$_3$ molecule were analyzed in numerous studies. However, most of them were devoted to the ground vibrational state, the deformational fundamentals ν_2 and

ν_4, and their overtones; see, e.g., the short review in Ref. (*8*). As to the stretching bands ν_1 and ν_3 and their overtones, there have been only a few studies, Refs. (*9–11*), where the rotational structure of the ν_1 and ν_3 fundamentals was discussed.

In our study, the high-resolution Fourier transform spectra of the PH$_3$ molecule are recorded in the wide spectral region 1750–9200 cm^{-1} (for illustration, the overview spectra of the $v = 1, 2, 3,$ and 4 ($v = \nu_1 + \nu_3$) polyads are shown in Fig. 1). In this case, because of the very complicated picture of spectra in regions of stretching overtone bands, as much initial information as possible about stretching fundamentals is desirable.

As mentioned above, the spectral region of 4–5 μm where the ν_1 and ν_3 bands are located was considered earlier in Refs. (*9–11*). The most careful analysis of the rotational structure of the ν_1 and ν_3 bands was made in (*11*). Unfortunately, even in that paper, information is absent on both the line positions and energy levels of the upper vibrational states. On the one hand, as our preliminary analysis shows, the set of parameters from (*11*) does not allow one to correctly describe numerous effects and peculiarities which appear in a high-resolution spectrum for transitions with quantum number $J > 10$. On the other hand, transitions with $J > 10$ are the most interesting and informative for understanding many resonance effects and the nature of different kinds of splitting in the spectrum of the PH$_3$ molecule in the region 4–5 μm.

So, in this contribution, we present the results (a) of a high-resolution reanalysis of the spectral region where the fundamental stretching bands ν_1 and ν_3 are located and (b) of the assignment of corresponding recorded transitions. Experimental

---

[1] At least, as discussed in Refs. (*6, 7*), the local mode effects clearly appear in spectra of stretching bands of the phosphine's deuterated species PH$_2$D and PHD$_2$.
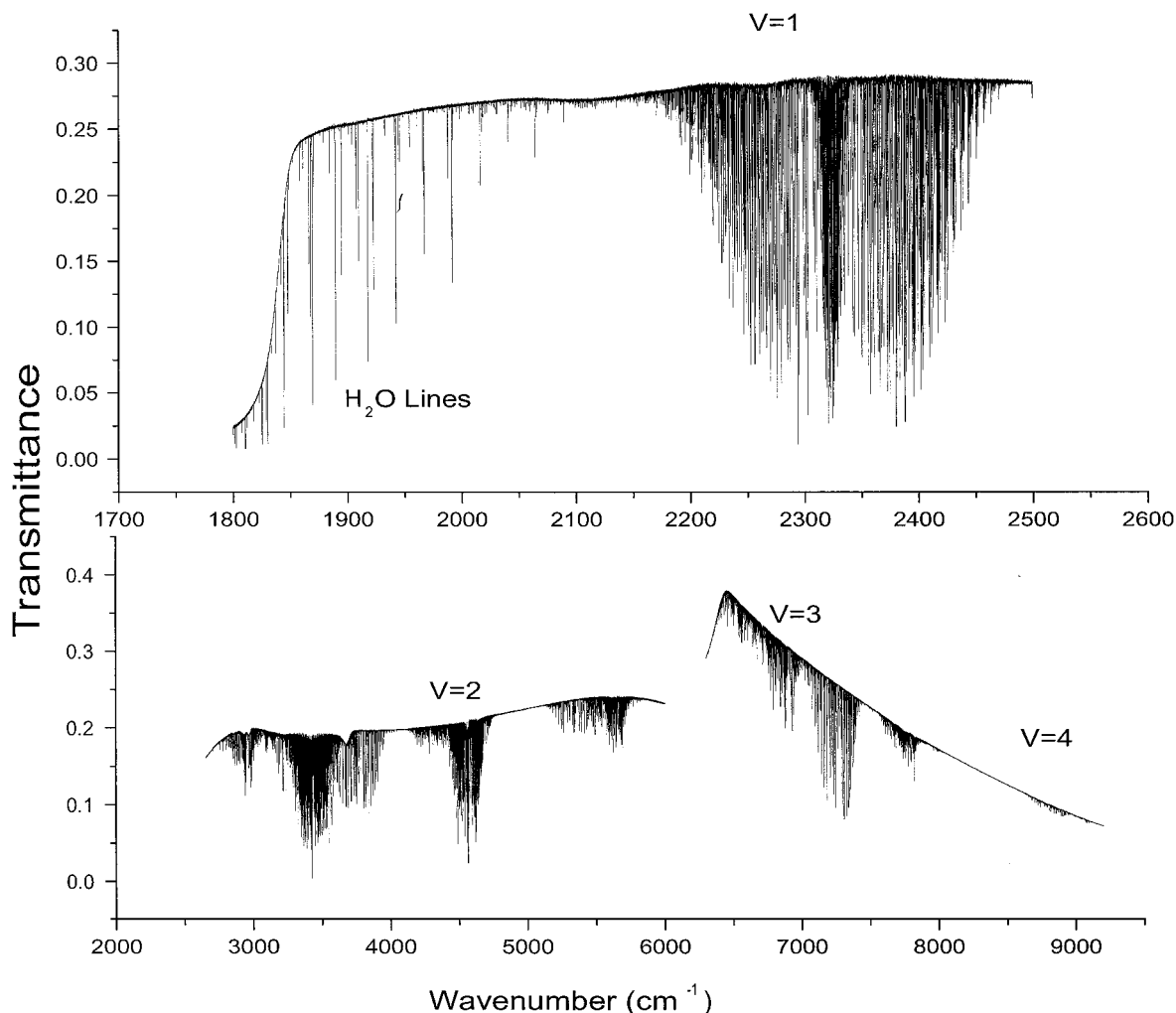
FIG. 1. Low-resolution Fourier transform spectra of PH_3.

details are reported in Section 2. It should be mentioned that transitions with the value of quantum number $J \leq 10$ can be assigned without any difficulties on the basis of the traditional ground state combination differences method. At the same time, assignment of transitions with $J > 10$ is not a trivial problem because of the presence of numerous and strong resonance interactions, on the one hand, and because of the decrease of linestrengths when the value of the quantum number J increases, on the other hand. Under these conditions, preliminary predictions for the line positions of transitions with $J > 10$ are very useful. For this reason, the assignments of transitions were carried out simultaneously with a fit of upper energies. The Hamiltonian used in the fit is briefly discussed in Section 3. Besides the ν_1 and ν_3, the $2\nu_4$ and $\nu_2 + \nu_4$ bands, which strongly perturb the rotational structure of the $(1000, A_1)$ and $(0010, E)$ vibrational states, were taken into consideration, as well. The very weak band $2\nu_2$ is not reanalyzed and its influence on the other bands is taken into account via the fitting of corresponding resonance interaction parameters. Assignments of the recorded

transitions and discussion of the appeared effects are presented in Section 4.

2. EXPERIMENTAL DETAILS

The PH_3 sample was purchased from the Nanjing Special Gas Company with a stated purity of 99.9%. The spectra are recorded at room temperature with a Bruker IFS 120HR Fourier-transform interferometer (Hefei, China), which is equipped with a path length adjustable multipass gas cell. The spectra are recorded in the region 1750–9200 cm^{-1} under different experimental conditions. The experimental details can be found in Table 1. In this paper we mainly discuss the spectra in the region 1750–2500 cm^{-1}, which includes ν_1, ν_3, $2\nu_4$, and $\nu_2 + \nu_4$ bands (two parts of the recorded high-resolution spectra are shown for illustration in Figs. 2 and 3). A CO_2 absorption band overlapping with the ν_1 and ν_3 bands of PH_3 is observed. These lines of CO_2 are used to calibrate the lines of PH_3 in the region 2100–2500 cm^{-1}. The lines of PH_3 in the longer wave region are

TABLE 1
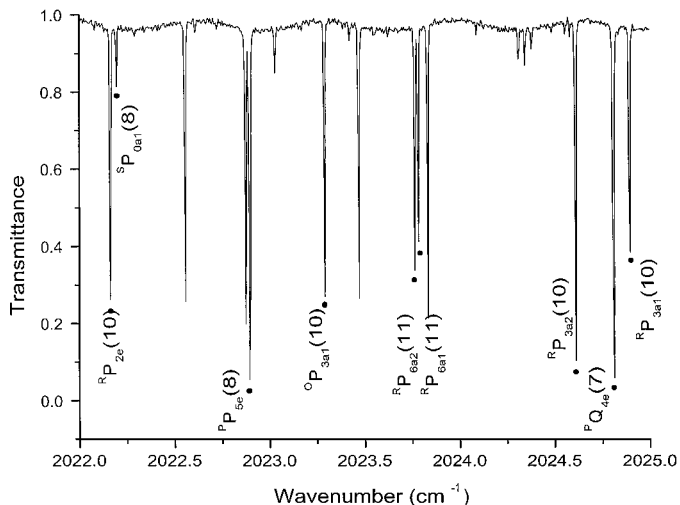### The Details of the Experimental Conditions

Region (cm^{-1})	Resolution (cm^{-1})	Pressure (Pa)	Path length (m)
1750–2500	0.005	37	15
2100–2500	0.005	257	0.1
2800–4000	0.005	40	15
4100–4750	0.010	1910	15
4100–4750	0.010	150	15
5000–6000	0.015	1969	15
6300–8100	0.015	4558	51
8500–9200	0.020	8960	105

FIG. 3. Portion of the $\nu_2 + \nu_4$ band of PH₃ in the P-branch region: resolution 0.005 cm^{-1}, pressure 37 Pa, path length 15 m.

calibrated with the H₂O lines. In this case, all the observed lines of CO₂ and H₂O are compared with those listed in the GEISA 97 database. The accuracy of the not very weak unblended and unsaturated lines is estimated to be not worse than 0.0003–0.0005 cm^{-1}.

3. HAMILTONIAN MODEL

The PH₃ molecule is a symmetric top with the value of the angles between the bonds close to 90°. Its stretching fundamental bands, ν_1 and ν_3, are very close to each other (near 2321.1 cm^{-1}

and 2326.9 cm^{-1}, respectively) and are located about two times higher in wavenumber than the deformational fundamental bands ν_2 and ν_4 (992.1348 cm^{-1} and 1118.3064 cm^{-1}, respectively, Ref. (8)). Taking into account that PH₃ is a light molecule with large enough values of rotational and centrifugal
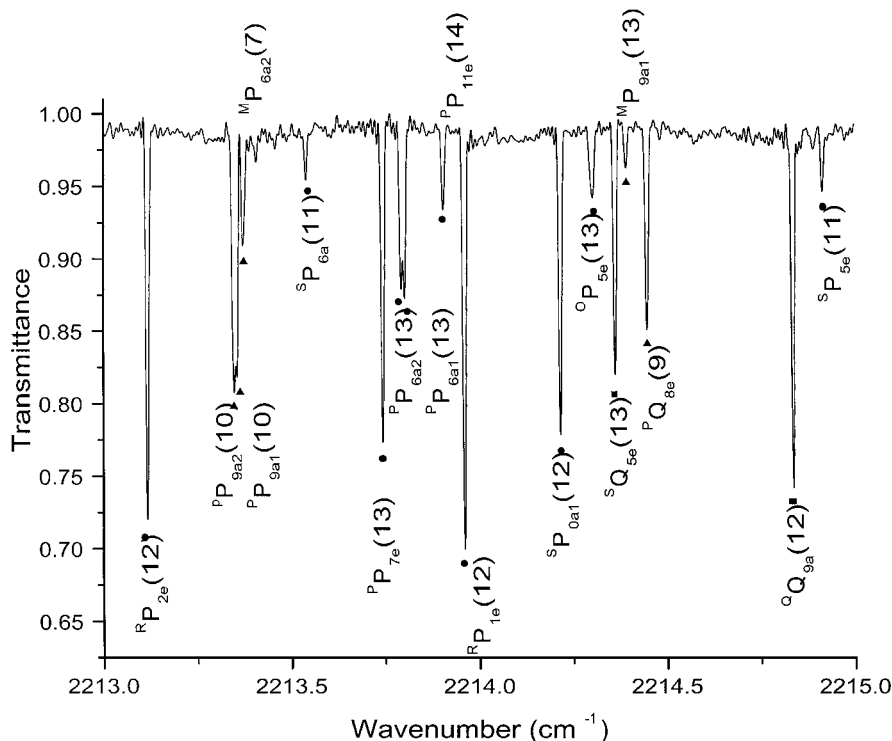
FIG. 2. Detail of the spectrum of PH₃ in the region of the ν_3 band: resolution 0.005 cm^{-1}, pressure 257 Pa, path length 0.1 m. Some lines belonging to the $2\nu_4$ band can also be seen.

distortion parameters ($B^{gr.} = 133.480\,110\,3$ GHz, $C^{gr.} = 117.489\,507\,9$ GHz, Ref. (8)), one should expect the appearance of numerous strong resonance interactions between all the states ($v_1 v_2 v_3 v_4$) which have the same value of the number $v(v = 2v_1 + v_2 + 2v_3 + v_4)$. As a consequence, one should expect that the correct description of the high-resolution spectra of the PH$_3$ molecule is possible only with a Hamiltonian description which would take into account different kinds of both Fermi and Coriolis-type interactions between all the states of a polyad $v = 2v_1 + v_2 + 2v_3 + v_4$.

In the present study, we used the Hamiltonian model which was derived in Ref. (12) on the basis of the symmetry properties of a molecule and which allows one to take into account any kinds of effects and interactions that appear in one or another polyad. That Hamiltonian has the form of the effective operator

$$H^{v.-r.} = \sum_{v,v'} H^{vv'}, \qquad [1]$$

where the summation is fulfilled in all the vibrational states of a poliad. In our case, $v, v' = 1, \ldots, 6$, and it is denoted: $|1\rangle = (0200, A_1)$, $|2\rangle = (0002, A_1)$, $|3\rangle = (1000, A_1)$, $|4\rangle = (0101, E)$, $|5\rangle = (0002, E)$, $|6\rangle = (0010, E)$. The diagonal operators H^{vv} describe rotational structures of corresponding vibrational states. The nondiagonal operators $H^{vv'}$ ($v \neq v'$), describe resonance interactions between the states $|v\rangle$ and $|v'\rangle$. In this case, for symmetric vibrational states (A_1 symmetry), the $H^{A_1 A_1}$ operators have the form

$$H^{A_1 A_1} = |A_1\rangle\langle A_1| \Bigg\{ E^a + B^a (J_x^2 + J_y^2) + C^a J_z^2 - D_J^a J^4$$
$$- D_{JK}^a J^2 J_z^2 - D_K^a J_z^4 + \cdots + \Bigg[\Bigg(\frac{1}{2}\epsilon^a + \frac{1}{2}\epsilon_J^a J^2$$
$$+ \epsilon_K^a J_z^2 + \cdots \Bigg), (J_+^3 - J_-^3) \Bigg]_+ + \Bigg[(\epsilon'^a J_z + \epsilon_J'^a J_z J^2$$
$$+ \epsilon_K'^a J_z^3 + \cdots), (J_+^3 + J_-^3) \Bigg]_+ \Bigg\}. \qquad [2]$$

Here the B^a, C^a, D_J^a, D_{JK}^a, D_K^a, ... are the rotational and centrifugal distortion parameters; operators $(J_+^3 - J_-^3)$ and $(J_+^3 + J_-^3)$ connect the rotational states $|JK\rangle$ and $|JK'\rangle$ which differ from each other by the value of the quantum number K, namely, $\Delta K = K - K' = \pm 3$. They provide, in particular, the a_1–a_2 splittings of levels with the quantum number $K = 3$. Parameters ϵ^a, ϵ_J^a, ϵ_K^a and ϵ'^a, $\epsilon_J'^a$, $\epsilon_K'^a$ describe the J and K dependencies of the main ϵ^a and $\bar{\epsilon}^a$ parameters. $[\ldots, \ldots]_+$ denotes the anticommutator.

For doubly degenerate vibrational states (E symmetry), the H^{EE} operator is

$$H^{EE} = H_1^{EE} + H_2^{EE} + H_3^{EE}, \qquad [3]$$

where

$$H_1^{EE} = (|E_1\rangle\langle E_1| + |E_2\rangle\langle E_2|) \Bigg\{ E^e + B^e (J_x^2 + J_y^2)$$
$$+ C^e J_z^2 - D_J^e J^4 - D_{JK}^e J^2 J_z^2 - D_K^e J_z^4 + \cdots$$
$$+ \Bigg[\Bigg(\frac{1}{2}\epsilon^e + \frac{1}{2}\epsilon_J^e J^2 + \epsilon_K^e J_z^2 + \cdots \Bigg), (J_+^3 - J_-^3) \Bigg]_+$$
$$+ \Bigg[(\epsilon'^e J_z + \epsilon_J'^e J_z J^2 + \epsilon_K'^e J_z^3 + \cdots), (J_+^3 + J_-^3) \Bigg]_+ \Bigg\}, \qquad [4]$$

$$H_2^{EE} = (|E_1\rangle\langle E_2| - |E_2\rangle\langle E_1|) \{ 2(C\zeta)J_z + \eta_J J_z J^2 + \eta_K J_z^3$$
$$+ \eta_{JJ} J_z J^4 + \eta_{JK} J_z^3 J^2 + \eta_{KK} J_z^5 + \eta_{JJJ} J_z J^6$$
$$+ \eta_{JJK} J_z^3 J^4 + \eta_{JKK} J_z^5 J^2 + \eta_{KKK} J_z^7 + \cdots \}, \qquad [5]$$

and

$$H_3^{EE} = (|E_2\rangle\langle E_2| - |E_1\rangle\langle E_1|) \{ [iA, (J_+ - J_-)]_+ + [B, (J_+$$
$$+ J_-)]_+ + [C, (J_+^2 + J_-^2)]_+ + [iD, (J_-^2 - J_+^2)]_+$$
$$+ [F, (J_+^4 + J_-^4)]_+ + [iG, (J_-^4 - J_+^4)]_+ \} + (|E_1\rangle\langle E_2|$$
$$+ |E_2\rangle\langle E_1|) \{ [A, (J_+ + J_-)]_+ + [iB, (J_- - J_+)]_+$$
$$+ [iC, (J_+^2 - J_-^2)]_+ + [D, (J_+^2 + J_-^2)]_+$$
$$+ [iF, (J_+^4 - J_-^4)]_+ + [G, (J_+^4 + J_-^4)]_+ \}, \qquad [6]$$

$$A = \frac{1}{2}\alpha + \frac{1}{2}\alpha_J J^2 + \alpha_K J_z^2 + \cdots,$$
$$B = \beta J_z + \beta_J J_z J^2 + \beta_K J_z^3 + \beta_{JJ} J_z J^4 + \beta_{JK} J^2 J_z^3 + \cdots,$$
$$C = \frac{1}{2}\gamma + \frac{1}{2}\gamma_J J^2 + \gamma_K J_z^2 + \frac{1}{2}\gamma_{JJ} J^4 + \gamma_{JK} J^2 J_z^2 + \cdots,$$
$$D = \delta J_z + \delta_J J_z J^2 + \delta_K J_z^3 + \delta_{JJ} J_z J^4 + \delta_{JK} J^2 J_z^3 + \cdots, \qquad [7]$$
$$F = \frac{1}{2}\kappa + \frac{1}{2}\kappa_J J_z^2 + \kappa_K J_z^4 + \frac{1}{2}\kappa_{JJ} J^4 + \kappa_{JK} J^2 J_z^2 + \cdots,$$
$$G = \theta J_z + \theta_J J_z J^2 + \theta_K J_z^3.$$

In Eq. [4] the E^e, B^e, ..., ϵ'^e, ... parameters have the same sense as the corresponding parameters in Eq. [2] with only one exception: operators $(J_+^3 \pm J_-^3)$ also connect to each other the rotational states $|JK\rangle$ and $|JK'\rangle$ with $\Delta K = K - K' = \pm 3$, but they do not split the a_1/a_2 levels. Operator H_2^{EE} describes the $k - l$ splittings; other operators, $(J_+^n \pm J_-^n)$, connect to each other the rotational states $|JK\rangle$ and $|JK'\rangle$ with $\Delta K = K - K' = \pm n$. In this case, the operators with $n = 2m$ provide the a_1–a_2 splittings of energy levels with $K = m$.

Resonance interaction operators can be divided into two types:

(1) Fermi-type operators which connect vibrational states of the same symmetry. In this case, corresponding $H^{v\Gamma,v'\Gamma'}$ operators have the form

$$H^{vA_1,v'A_1} = |vA_1\rangle\langle v'A_1| \left\{ F_0^{v-v'} + F_J^{v-v'}\left(J_x^2 + J_y^2\right) \right.$$

$$+ F_K^{v-v'} J_z^2 - F_{JJ}^{v-v'} J^4 - F_{JK}^{v-v'} J^2 J_z^2 + \cdots$$

$$+ \left[\left(\frac{1}{2}\tilde{\epsilon}^a + \frac{1}{2}\tilde{\epsilon}_J^a J^2 + \tilde{\epsilon}_K^a J_z^2 + \cdots \right), (J_+^3 - J_-^3) \right]_+$$

$$\left. + \left[(\tilde{\epsilon}'^a J_z + \tilde{\epsilon}'^a_J J_z J^2 + \tilde{\epsilon}'^a_K J_z^3 + \cdots), (J_+^3 + J_-^3) \right]_+ \right\}$$

$$[8]$$

and

$$H^{vE,v'E} = H_1^{vE,v'E} + H_2^{vE,v'E} + H_3^{vE,v'E}, \qquad [9]$$

$$H_1^{vE,v'E} = (|E_1\rangle\langle E_1| + |E_2\rangle\langle E_2|) \left\{ F_0^{v-v'} + F_J^{v-v'}\left(J_x^2 + J_y^2\right) \right.$$

$$+ F_K^{v-v'} J_z^2 - F_{JJ}^{v-v'} J^4 - F_{JK}^{v-v'} J^2 J_z^2 - F_{KK}^{v-v'} J_z^4 + \cdots$$

$$+ \left[\left(\frac{1}{2}\tilde{\epsilon}^e + \frac{1}{2}\tilde{\epsilon}_J^e J^2 + \tilde{\epsilon}_K^e J_z^2 + \cdots \right), (J_+^3 - J_-^3) \right]_+$$

$$\left. + \left[(\tilde{\epsilon}'^e J_z + \tilde{\epsilon}'^e_J J_z J^2 + \tilde{\epsilon}'^e_K J_z^3 + \cdots), (J_+^3 + J_-^3) \right]_+ \right\},$$

$$[10]$$

$$H_2^{vE,v'E} = (|E_1\rangle\langle E_2| - |E_2\rangle\langle E_1|) \left\{ 2(\tilde{C}\zeta)J_z + \tilde{\eta}_J J_z J^2 + \tilde{\eta}_K J_z^3 \right.$$

$$+ \tilde{\eta}_{JJ} J_z J^4 + \tilde{\eta}_{JK} J_z^3 J^2 + \tilde{\eta}_{KK} J_z^5 + \tilde{\eta}_{JJJ} J_z J^6$$

$$\left. + \tilde{\eta}_{JJK} J_z^3 J^4 + \tilde{\eta}_{JKK} J_z^5 J^2 + \tilde{\eta}_{KKK} J_z^7 + \cdots \right\},$$

$$[11]$$

$$H_3^{vE,v'E} = (|E_2\rangle\langle E_2| - |E_1\rangle\langle E_1|)\{[i\tilde{A}, (J_+ - J_-)]_+ + [\tilde{B}, (J_+$$

$$+ J_-)]_+ + [\tilde{C}, (J_+^2 + J_-^2)]_+ + [i\tilde{D}, (J_-^2 - J_+^2)]_+$$

$$+ [\tilde{F}, (J_+^4 + J_-^4)]_+ + [i\tilde{G}, (J_-^4 - J_+^4)]_+\}$$

$$+ (|E_1\rangle\langle E_2| + |E_2\rangle\langle E_1|)\{[\tilde{A}, (J_+ + J_-)]_+$$

$$+ [i\tilde{B}, (J_- - J_+)]_+ + [i\tilde{C}, (J_+^2 - J_-^2)]_+$$

$$+ [\tilde{D}, (J_+^2 + J_-^2)]_+ + [i\tilde{F}, (J_+^4 - J_-^4)]_+$$

$$+ [\tilde{G}, (J_+^4 + J_-^4)]_+\}. \qquad [12]$$

Here the operators $\tilde{A}, \tilde{B}, \ldots$, etc., can be derived from Eq. [7] by substitution of the parameters $\tilde{\alpha}, \tilde{\beta}, \ldots$, etc., for the parameters $\alpha, \beta, \ldots$.

(2) Coriolis-type resonance operators which connect vibrational states of different symmetries, A_1 and E. In this case,

$$H^{vA_1v'E} = |A_1\rangle\langle E_1|\{[iA^*, (J_+ - J_-)]_+ + [B^*, (J_+ + J_-)]_+$$

$$+ [C^*, (J_+^2 + J_-^2)]_+ + [iD^*, (J_-^2 - J_+^2)]_+$$

$$+ [F^*, (J_+^4 + J_-^4)]_+ + [iG^*, (J_-^4 - J_+^4)]_+\}$$

$$+ |A_1\rangle\langle E_2|\{[A^*, (J_+ + J_-)]_+ + [iB^*, (J_- - J_+)]_+$$

$$+ [iC^*, (J_+^2 - J_-^2)]_+ + [D^*, (J_+^2 + J_-^2)]_+$$

$$+ [iF^*, (J_+^4 - J_-^4)]_+ + [G^*, (J_+^4 + J_-^4)]_+\}. \qquad [13]$$

As in the case of the Fermi-type interaction, the operators A^*, $B^*, \ldots$, etc., can be derived from Eq. [7] by substitution of the parameters $\alpha^*, \beta^*, \ldots$, etc., for the parameters $\alpha, \beta, \ldots$.

4. DESCRIPTION OF THE SPECTRUM AND ASSIGNMENT OF TRANSITIONS

As shown in Figs. 1 and 4 (Fig. 4 shows the diagram of the rovibrational energies for all vibrational states of the considered polyad), the strongest parallel band ν_1 and perpendicular band ν_3 are totally overlapped and located about 100 cm⁻¹ and 200 cm⁻¹ higher than the nearest and considerably weaker bands $2\nu_4$ and $\nu_2 + \nu_4$, respectively. For this reason, transitions belonging to the upper states with low values of quantum number J ($J < 10$) can be assigned without large difficulties for all the bands if one takes into account the Coriolis resonance interaction between the $(1000, A_1)$ and $(0010, E)$ states, on the one hand, and the $(0002, A_1)$ and $(0002, E)$ states, on the other hand. At the same time, beginning from $J = 10$, strong overlaps and, as a consequence, strong perturbations can be seen for the
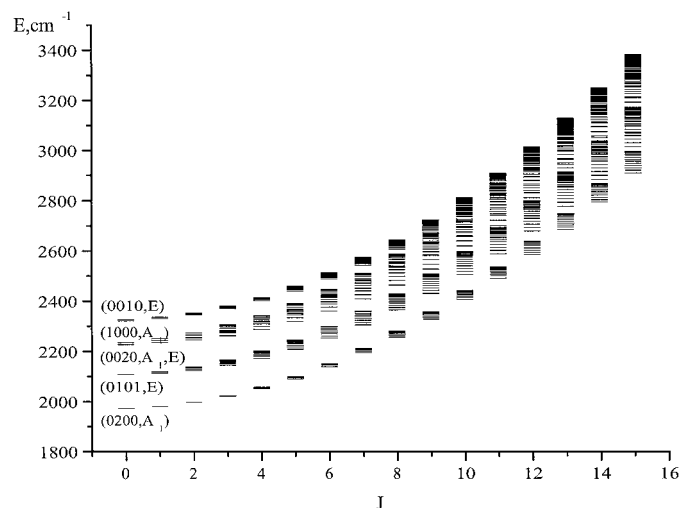
FIG. 4. The diagram of the rovibrational energies for the vibrational states $(0200, A_1)$, $(0101, E)$, $(0002, A_1, E)$, $(1000, A_1)$, and $(0010, E)$ of the PH₃ molecule.
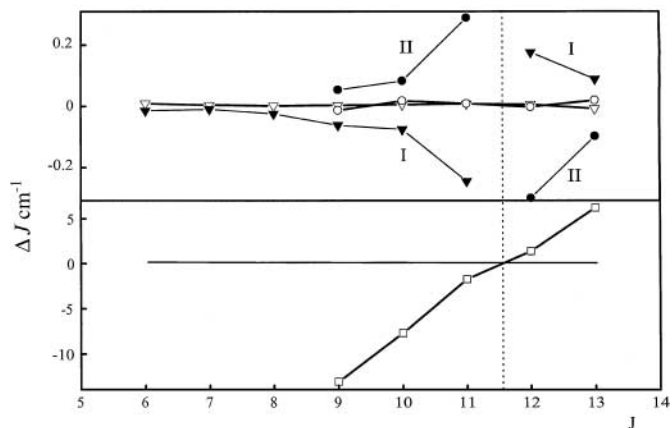
FIG. 5. Upper part: Dependence of the differences $\Delta_{(J)} = E_{JK}^{exp.} - E_{JK}^{calc.}$ on the value of quantum number J for the states $[JK = 6e](0002, E)$ (curve I) and $[JK = 9e](0010, E)$ (curve II). The dark triangles and circles belongs to the $\Delta_{(J)}$-differences, which are calculated in the absence of resonance operators in the Hamiltonian. When the resonance interactions between the states $(0002, E)$ and $(0010, E)$ are taken into account, the plots of the $\Delta_{(J)}$-differences are transformed to those marked by open triangles and circles. The bottom part of the figure shows the plot of the dependence of the difference $E_{[JK = 6e](0002, E)} - E_{[JK = 9e](0010, E)}$ on the value of the quantum number J, which explains the behavior of the $\Delta_{(J)}$ values on the upper part of the figure.

states $(0002, A_1)$, $(0002, E)$, and the set of states $(1000, A_1)$, $(0010, E)$, and $(0101, E)$. As illustration of such resonance interactions, the upper part of Fig. 5 gives the plots of dependencies of the differences $\Delta_{(J)} = E_{JK}^{exp.} - E_{JK}^{calc.}$ against the value of the quantum number J for the states $[JK = 6e](0002, E)$ (curve I) and $[JK = 9e](0010, E)$ (curve II), respectively. In this case, dark triangles and circles belong to the $\Delta_{(J)}$-differences which were calculated in the absence of corresponding resonance operators in the Hamiltonian. From this figure, one can see that the situation appears near the values of the quantum number $J = 11$ and 12, which is typical for resonance interactions. In this case, as one can see from the lower part of Fig. 5, just between these values of quantum number J, the plot of the dependence of the difference of energies $E_{[JK=6e](0002, E)} - E_{[JK=9e](0010, E)}$ crosses the "zero" line. At the same time, if one takes into account the resonance interactions of the $(J_+^3 \pm J_-^3)$ type (see Sect. 3) between the states $(0002, E)$ and $(0010, E)$, the plots of the dependencies of the $\Delta_{(J)}$-differences on the value of the quantum number J are transformed to those marked by open triangles and circles.

Assignment of the spectrum was made on the base of the ground state combination differences method, and the ground state energies were calculated with the parameters from Ref. (8). In this case, as already mentioned above, transitions with quantum number $J \leq 10$ were assigned without large difficulty for all the studied bands. At the same time, assignments of transitions with $J > 10$ met two problems. First, many rovibrational states of $(1000, A_1)$ and $(0010, E)$ are strongly perturbed by the rovibrational states of the $(0002, A_1, E)$ and even $(0101, E)$. As a consequence, an assignment of transitions with higher values
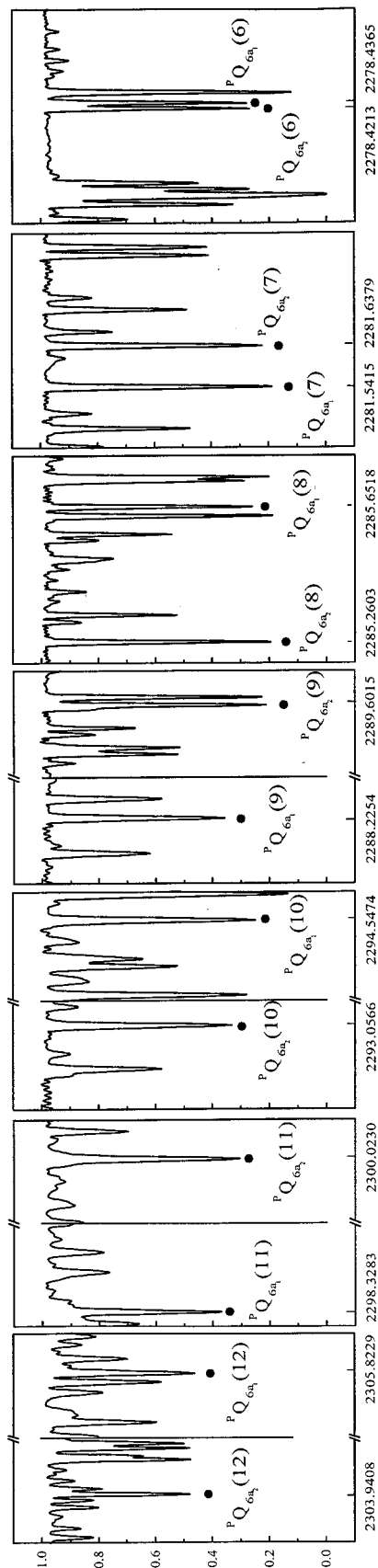

FIG. 6. A set of Q-branch transitions leading to the split $[J^{upper} K^{upper} = 5a_1/a_2]$ states of the $2\nu_4(E)$ band of PH_3.

TABLE 2
Experimental Rovibrational Term Values for the (0010, E), (0101, E), and (0002, E) Vibrational States of the PH$_3$ Molecule (in cm^{-1})[a]

		(0010, E)		(0002, E)		(0101, E)				(0010, E)		(0002, E)		(0101, E)	
J K Γ		E	Δ	E	Δ	E	Δ	J K Γ		E	Δ	E	Δ	E	Δ
1		2	3	4	5	6	7	1		2	3	4	5	6	7
0 0 E		2326.8664		2234.9330		2108.1514		6 2 E		2509.6152	6	2415.7307	13	2296.8978	4
1 1 A1		2335.0459		2236.3808		2120.0770		6 1 A$_1$		2511.1202	2	2424.4457	5	2295.9194	4
1 1 A2		2335.0348	2	2236.4531		2120.2650	2	6 1 A$_2$		2511.3560		2424.4842	6	2291.7779	4
1 0 E		2335.6844	1	2244.2260	3	2116.8262	2	6 0 E		2511.8724	4	2431.6952	6	2289.9393	8
1 1 E		2335.3222	6	2250.5123		2112.6465		6 1 E		2511.5142	4	2437.4267	12	2286.1579	2
2 2 E		2351.0243	2	2245.5644	9	2140.0337	3	6 2 A$_1$		2510.2394	3	2443.2608	19	2281.3302	2
2 1 A$_1$		2352.6586	1	2255.1932		2137.8003	2	6 2 A$_2$		2510.1063	3	2440.7311	9	2281.2880	4
2 1 A$_2$		2352.6921	2	2255.0020	3	2137.2326		6 3 E		2507.0105	4	2445.1596	3	2275.5209	2
2 0 E		2353.3182	4	2262.8670	2	2134.1724	4	6 4 E		2504.6182	8	2446.3299	2	2268.8202	8
2 1 E		2352.9564	4	2269.1507	5	2130.0074	2	6 5 A$_1$		2500.0457	4	2446.0829	9	2261.2103	7
2 2 A$_1$		2351.5930	5			2124.9859	2	6 5 A$_2$		2500.0457	4	2446.0670	10	2261.2103	7
2 2 A$_2$		2351.5912	13	2273.8205	4	2124.9859	2	6 6 E		2494.7566	8	2444.1564	10	2252.6908	2
3 3 E		2375.6754	2	2262.4982	3	2167.7172	1	7 7 A$_1$		2547.5985	7	2407.5618	13	2356.4933	5
3 2 E		2377.4751	7	2273.4685	10	2166.0813	1	7 7 A$_2$		2547.5985	7	2407.5618	13	2356.4933	5
3 1 A$_1$		2379.1551	1	2283.0536	2	2162.9733	6	7 6 E		2556.3733	8	2424.7645	15	2358.2063	5
3 1 A$_2$		2379.0879	3	2283.2551	5	2164.1205	1	7 5 E		2560.5619	4	2449.7851	9	2359.4274	11
3 0 E		2379.7619	2	2290.8961	12	2160.1788	3	7 4 A$_1$		2565.0808	5	2461.8138	7	2359.6654	6
3 1 E		2379.4010	6	2297.1525	3	2156.0483	4	7 4 A$_2$		2565.0808	5	2461.8138	7	2359.6990	3
3 2 A$_1$		2378.0349	5	2301.7070	7	2151.0421	5	7 3 E		2569.4811	4	2472.5320	8	2359.3047	4
3 2 A$_2$		2378.0445	5	2301.9262	3	2151.0421	5	7 2 E		2571.2158	10	2481.9143	17	2358.1388	12
3 3 E		2374.8149	7	2304.8961	16	2145.1674		7 1 A$_1$		2572.9845		2490.4292	13	2351.9255	2
4 4 A$_1$		2406.4143	5	2287.1715	14	2203.2190	9	7 1 A$_2$		2572.6791	29	2490.4214	21	2357.4734	3
4 4 A$_2$		2406.4143	5	2287.1715	14	2203.2190	9	7 0 E		2573.4620	3	2497.3198	11	2350.3575	3
4 3 E		2410.9382	3	2299.6968	7	2202.4246	2	7 1 E		2573.1063	3	2502.6738	1	2346.7918	16
4 2 E		2412.7314	4	2311.1641	7	2200.8793	3	7 2 A$_1$		2571.6583	3	2505.3686	3	2342.0183	3
4 1 A$_1$		2414.3143	3	2320.7193	4	2199.2399	2	7 2 A$_2$		2571.8851	4	2509.3782	5	2342.0928	3
4 1 A$_2$		2414.4272	8	2320.6458	33	2197.3065	3	7 3 E		2568.6401	6	2510.9560	5	2336.3349	2
4 0 E		2415.0096	7	2328.3780	7	2194.8269	5	7 4 E		2566.3036	12	2511.8204	9	2329.6775	5
4 1 E		2414.6488	7	2334.5493	5	2190.7632	5	7 5 A$_1$		2561.5709	4	2511.4282	2	2322.0953	3
4 2 A$_1$		2413.3078	5	2339.4814	7	2185.7894	2	7 5 A$_2$		2561.5709	4	2511.5244	2	2322.0953	3
4 2 A$_2$		2413.2773	3	2338.8479	2	2185.7823	9	7 6 E		2555.1727	4	2509.2857	6	2313.5908	4
4 3 E		2410.0854	2	2342.2081	3	2179.9259	2	7 7 E		2550.0554	7	2505.8899		2304.1565	3
4 4 E		2407.5910	2	2343.6564	2	2173.1844		8 8 E		2610.2666					
5 5 E		2445.8504	5	2319.5760	5	2246.5328	5	8 7 A$_1$		2617.8246	6	2481.8921	5	2425.7445	6
5 4 A$_1$		2450.5144	3	2333.6589	13	2246.5857	2	8 7 A$_2$		2617.8246	6	2481.8921	5	2425.7445	6
5 4 A$_2$		2450.5144	3	2333.6589	13	2246.5857	2	8 6 E		2626.7245	6	2512.3261	13	2427.5819	8
5 3 E		2454.1544	3	2348.3953	6	2245.8845	3	8 5 E		2631.0682	8	2525.8272	11	2429.2303	9
5 2 E		2456.7829	10	2358.6925	3	2244.4741	4	8 4 A$_1$		2635.5166	11	2537.7163	9	2429.5793	4
5 1 A$_1$		2458.4985		2367.8285	4	2240.2398	5	8 4 A$_2$		2635.5166	11	2537.7163	9	2429.4714	8
5 1 A$_2$		2458.3290	2	2367.8078	9	2243.1714	2	8 3 E		2639.8558	5	2548.1905	9	2429.3456	8
5 0 E		2459.0500	6	2375.3328	16	2238.0891	10	8 2 E		2641.5647	6	2557.6876	11	2428.1284	8
5 1 E		2458.6904	6	2381.3348	4	2234.1394	2	8 1 A$_1$		2642.9869	3	2565.5303	2	2427.7989	3
5 2 A$_1$		2457.3064	3	2385.2054	6	2229.2018	3	8 1 A$_2$		2643.3661		2565.4768	5	2420.6813	2
5 2 A$_2$		2457.3757	3	2386.5930	4	2229.2232	3	8 0 E		2643.8029	11	2572.0303	11	2419.3370	17
5 3 E		2455.0024	4	2388.9253	9	2223.3795	1	8 1 E		2643.4512	9	2576.9077	10	2416.0168	10
5 4 E		2451.7057	4	2390.2936	8	2216.6518	3	8 2 A$_1$		2642.2896	5	2584.7014	5	2411.4856	2
5 5 A$_1$		2447.2398	2	2390.1079		2209.0288	4	8 2 A$_2$		2641.9407	13	2579.0616	5	2411.3671	2
5 5 A$_2$		2447.2398	2	2390.1079		2209.0288	4	8 3 E		2639.0260	2	2586.2744	11	2405.7978	9
6 6 E		2492.5497	17	2359.7084	20	2297.5978	2	8 4 E		2636.7326	8	2586.8219	9	2399.2050	9
6 5 E		2498.8175	3	2375.3503	9	2298.5627	2	8 5 A$_1$		2631.7847	12	2586.6076	4	2391.6679	10
6 4 A$_1$		2503.4073	5	2388.5319	7	2298.7233	21	8 5 A$_2$		2631.7847	12	2586.2164	4	2391.6679	10
6 4 A$_2$		2503.4073	5	2388.5319	7	2298.7185	3	8 6 E		2625.7425	9	2583.7486	9	2383.1930	7
6 3 E		2507.8553	6	2405.8875	7	2298.1698	8	8 7 E		2620.4883	2	2580.3816	15	2373.7774	8

[a] In Table 2, Δ is the experimental uncertainty of the energy value, equal to one standard deviation in units of 10^{-4} cm^{-1}. The Δ is not quoted when the energy value was obtained from only one transition. Such energies were not used in the fit and they can be considered as a prediction.

TABLE 2—*Continued*

J	K	Γ	(0010, E) E	Δ	(0002, E) E	Δ	(0101,E) E	Δ	J	K	Γ	(0010,E) E	Δ	(0002,E) E	Δ	(0101,E) E	Δ
		1	2	3	4	5	6	7			1	2	3	4	5	6	7
8	8	A$_1$	2613.1752		2575.2138		2363.4097	13	11	11	E	2844.4180				2668.9195	8
8	8	A$_2$	2613.1752		2575.2138		2363.4097	13	11	10	A$_1$	2855.2322	4			2674.5998	5
9	9	E	2684.1278				2497.4663	6	11	10	A$_2$	2855.2322	4			2674.5998	5
9	8	E	2689.2850	4	2546.7245	3	2500.9939	2	11	9	E	2869.1954	12	2746.0914		2679.2666	3
9	7	A$_1$	2696.7563	11			2503.7862	20	11	8	E	2873.3165	7	2764.4793	10	2683.1933	3
9	7	A$_2$	2696.7563	11			2503.7862	20	11	7	A$_1$	2880.6351	9	2780.6748	7	2686.3643	10
9	6	E	2705.7723	6	2597.6652	6	2505.7806	5	11	7	A$_2$	2880.6351	9	2780.6748	7	2686.3299	3
9	5	E	2710.3162	3	2610.9129	9	2508.0885	4	11	6	E	2889.8432	6	2794.9512	12	2688.7222	6
9	4	A$_1$	2714.6947	18	2622.5574	24	2508.1629	7	11	5	E	2894.9515	7	2807.4250	3	2692.9507	14
9	4	A$_2$	2714.6947	18	2622.5574	24	2508.4428	2	11	4	A$_1$	2899.1990	6	2819.6880	10	2692.2248	11
9	3	E	2718.9531	10	2632.4095	9	2508.2955	11	11	4	A$_2$	2899.1251	10	2819.4863	11	2691.0288	4
9	2	E	2720.6424	8	2641.9943	11	2506.7703	8	11	3	E	2903.1928	9	2828.8821	7	2692.5574	6
9	1	A$_1$	2722.4788		2649.4678	4	2498.0422	15	11	2	E	2904.8864	10	2837.1220	8	2690.3285	7
9	1	A$_2$	2722.0510	4	2649.6056	4	2506.8372	4	11	1	A$_1$	2906.8192	7	2843.7712		2678.5358	4
9	0	E	2722.8770	6	2655.6616	10	2496.8735	9	11	1	A$_2$	2906.4611	5	2844.1291	4		
9	1	E	2722.5320	9	2660.0157	9	2493.8053	10	11	0	E	2907.1463	12	2849.2544	9	2677.6155	8
9	2	A$_1$	2720.9323	7	2661.7618	5	2489.3047	5	11	1	E	2906.8381	6	2852.6766	5	2675.0069	5
9	2	A$_2$	2721.4179	4	2671.3992	13	2489.4792	2	11	2	A$_1$	2904.9334	9	2854.5245	19	2670.8372	3
9	3	E	2718.1496	7	2671.4004	5	2483.8813	15	11	2	A$_2$	2905.6486	8	2869.1139	5	2671.1475	5
9	4	E	2715.8803	8	2670.9555	10	2477.3746	8	11	3	E	2902.5169	10	2868.8207	6	2665.7866	8
9	5	A$_1$	2710.6608	10	2670.4311	4	2469.9007	7	11	4	E	2900.2053	19	2867.9651	12	2659.5131	7
9	5	A$_2$	2710.6608	10	2669.0548	6	2469.9007	7	11	5	A$_1$	2894.3108	7	2866.8990	9	2652.2266	8
9	6	E	2705.0492	13	2667.5668	13	2461.4748	9	11	5	A$_2$	2894.3046	3	2865.2037	8	2652.2266	8
9	7	E	2699.6452	3	2664.0950	9	2452.0950	2	11	6	E	2889.7946	7	2863.1222	6	2643.9513	17
9	8	A$_1$	2692.4279	7	2658.9337	2	2441.7546	4	11	7	E	2884.0683	9	2859.1424	9	2634.6986	4
9	8	A$_2$	2692.4279	7	2658.9413	8	2441.7546	4	11	8	A$_1$	2877.1586	6	2853.2517	7	2624.4660	10
9	9	E	2680.6312		2652.0352		2430.4328		11	8	A$_2$	2877.1586	6	2853.8613	20	2624.4660	10
10	10	A$_1$	2758.6877	2	2597.4191	19	2579.4803	9	11	9	E	2864.8535	3	2846.9806	4	2613.2413	
10	10	A$_2$	2758.6877	2	2597.4191	19	2579.4803	9	11	10	E	2860.1323	12	2838.4508	10	2601.0072	7
10	9	E	2772.2438	6	2619.2728	36	2583.9563	7	11	11	A$_1$	2849.8850	11	2827.9714	24	2587.7257	
10	8	E	2776.9771	5	2660.5149	17	2587.6778	1	11	11	A$_2$	2849.8850	11	2827.9714	24	2587.7257	
10	7	A$_1$	2784.3699	11	2677.2329	12	2590.6387	10	12	11	E	2949.6997					
10	7	A$_2$	2784.3699	11	2677.2329	12	2590.6575	5	12	10	A$_1$	2960.3869	1			2778.5284	11
10	6	E	2793.4869	4	2691.9291	3	2592.8230	6	12	10	A$_2$	2960.3869	1			2778.5284	11
10	5	E	2798.2845	5	2704.8580	4	2595.8928	4	12	9	E	2969.8490	15	2859.3681	5	2783.4185	10
10	4	A$_1$	2802.5805	3	2716.0372	4	2594.5667	10	12	8	E	2978.2704	2	2877.0948	12	2787.2945	10
10	4	A$_2$	2802.5993	2	2716.1063	11	2595.7504	3	12	7	A$_1$	2985.5242	16	2892.7563	35	2790.8593	7
10	3	E	2806.7414	8	2726.7342	19	2596.1788	6	12	7	A$_2$	2985.5242	16	2892.7563	35	2790.9176	11
10	2	E	2808.4257	11	2735.1853	10	2594.1434	9	12	6	E	2995.2053	12	2906.5012	8	2793.4782	6
10	1	A$_1$	2809.8765	2	2742.5081	9			12	5	E	3000.2957	10	2917.4569	28		
10	1	A$_2$	2810.3066	3	2742.2555	6	2583.9977	2	12	4	A$_1$	3004.6617	6	2930.3708	9	2796.2619	9
10	0	E	2810.6649	5	2748.0941	12	2582.9688	15	12	4	A$_2$	3004.4767	5	2930.5145	15	2797.5601	13
10	1	E	2810.3328	6	2751.9447	3	2580.1421	3	12	3	E	3007.7043	13	2939.7768	9		
10	2	A$_1$	2809.2184	11	2765.6520	10	2576.0429	4	12	2	E	3009.9919	11	2947.7194	9		
10	2	A$_2$	2808.6051	9	2753.4658	9	2575.8029	4	12	1	A$_1$	3010.6920	7	2954.3885	14		
10	3	E	2805.9885	5	2765.4926	3	2570.5561	6	12	1	A$_2$	3011.9940	2	2954.0257		2781.6416	2
10	4	E	2803.7124	8	2764.8601	4	2564.1551	5	12	0	E	3012.3051	10	2959.1066	15	2780.8042	10
10	5	A$_1$	2798.1757	14	2762.5353	11	2556.7654	2	12	1	E	3012.0349	4			2778.3866	3
10	5	A$_2$	2798.1757	14	2764.0278	11	2556.7654	2	12	2	A$_1$	3011.7823	11	2981.5174	6	2774.7635	6
10	6	E	2793.0714	4	2760.7192	6	2548.4059	8	12	2	A$_2$	3009.8878	10	2962.8599	10	2774.3838	10
10	7	E	2787.5074	6	2757.0592	8	2539.0802	11	12	3	E	3008.2835	8	2981.2535	4	2769.5436	4
10	8	A$_1$	2780.4169	2	2751.8058		2528.7845	7	12	4	E	3005.3372	18	2980.1637	7	2763.4151	3
10	8	A$_2$	2780.4169	2	2751.7348	12	2528.7845	7	12	5	A$_1$	3001.5677	15	2976.9273	13	2756.2475	16
10	9	E	2768.4178	24	2744.9555	6	2517.5044	12	12	5	A$_2$	3001.5749	13	2978.8078	12	2756.2475	16
10	10	E	2762.9638		2736.3177	11	2505.2049		12	6	E	2994.8250	11	2975.4770	10	2748.0745	3

TABLE 2—*Continued*

J K Γ	(0010, E) E	Δ	(0002, E) E	Δ	(0101, E) E	Δ	J K Γ	(0010, E) E	Δ	(0002, E) E	Δ	(0101, E) E	Δ
1	2	3	4	5	6	7	1	2	3	4	5	6	7
12 7 E	2989.3658	12			2738.9102	4	14 14 E	3148.2489	10				
12 8 A$_1$	2982.8463	8			2728.7562	2	14 13 A$_1$	3161.8896	8				
12 8 A$_2$	2982.8016	7			2728.7562	2	14 13 A$_2$	3161.8896	8				
12 9 E	2974.0972				2717.6053	17	14 12 E	3174.7591					
12 10 E	2965.9190	11			2705.4419		14 11 E	3191.9350	22	3071.9668	8		
12 11 A$_1$	2956.0458	24			2692.2394	12	14 10 A$_1$	3202.4552	16	3092.8080	4		
12 11 A$_2$	2956.0458	24			2692.2394	12	14 10 A$_2$	3202.3887	12	3092.8080	4		
13 13 A$_1$	3039.0786						14 9 E	3211.4513	8				
13 13 A$_2$	3039.0786						14 8 E	3219.4759	11	3127.6135			
13 12 E	3051.9859	20					14 7 A$_1$	3226.3229	21	3141.0821	10		
13 11 E	3063.6766	15	2940.1102	7			14 7 A$_2$	3226.3835	18	3141.0821	10		
13 10 A$_1$	3074.1920	14	2961.8740	10			14 6 E			3156.9007	8		
13 10 A$_2$	3074.1920	14	2961.8740	10			14 5 E	3237.1994	7				
13 9 E	3083.5389	11	2981.1490	3			14 4 A$_1$	3241.2589	9				
13 8 E	3091.7831	22	2998.2124	4			14 4 A$_2$	3241.1367					
13 7 A$_1$	3099.0264	28	3013.2466	13			14 3 E	3243.9506	11				
13 7 A$_2$	3099.0264	28	3013.2466	13			14 1 A$_1$	3246.6184	9				
13 6 E	3109.3256	10	3025.5500	14			14 1 A$_2$	3248.2837	29				
13 5 E	3114.3243	14	3039.8634	6			14 0 E	3248.7236	13				
13 4 A$_1$	3118.4285	5	3050.2555	7			14 1 E	3248.5021	12				
13 4 A$_2$	3118.5432	8	3050.2679	5			14 2 A$_1$	3248.6580	19	3232.4182	9		
13 3 E	3122.0123	8					14 2 A$_2$			3258.3354	6		
13 2 E	3123.7148	23					14 3 E	3244.4544	31				
13 1 A$_1$	3125.8144	8	3072.8882	17			14 4 E	3241.6449	12				
13 1 A$_2$	3124.3441	8	3073.2689	11			14 8 A$_1$	3221.4427	7				
13 0 E	3126.1497	10			2892.5175	11	14 8 A$_2$	3221.5473					
13 1 E	3125.9188	4			2890.2659	9	14 10 E	3205.2630	8				
13 2 A$_1$	3123.4415	5					14 11 A$_1$	3195.5495	17				
13 2 A$_2$	3125.8271	7	3103.0021	22			14 11 A$_2$	3195.5495	17				
13 3 E	3121.5179	12	3102.3704	7			14 12 E	3185.3661	13				
13 4 E	3119.1135	11			2875.8237	9	14 13 E	3174.2455					
13 5 A$_1$	3115.3787	18					14 14 A$_1$	3163.1247	22				
13 5 A$_2$	3115.3889	18					14 14 A$_2$	3163.1247	22				
13 6 E	3110.8010	15	3095.5386	20	2860.7343	3	15 11 E			3212.0411	10		
13 7 E	3103.8380	9			2851.6738	6	15 4 A$_2$	3372.1787	29				
13 8 A$_2$	3096.1419	4					15 2 E	3377.5479					
13 9 E	3089.3338						15 1 A$_1$	3379.5941					
13 10 E	3080.9195						15 1 A$_2$	3377.8858					
13 11 A$_1$	3071.2672	7					15 0 E	3380.5545	16				
13 11 A$_2$	3071.2672	7					15 1 E	3380.0002	17				
13 12 E	3060.6644	28					15 2 A$_2$	3380.7663	27				
13 13 E	3049.3010	−56					15 4 E	3372.0290	32				

of the quantum number J was possible only simultaneously with the fitting of all upper energy levels. Second, transitions belonging to the $2\nu_4$ and $\nu_2 + \nu_4$ bands begin to be very weak for the upper states with $J > 10$. For this reason, only transitions to such upper states which are strongly perturbed by the rovibrational states of the ν_3 and ν_1 bands can be assigned without doubt.

Finally, we assigned more than 700, 1500, 600, 950, and 750 transitions to the ν_1, ν_3, $2\nu_4(A_1)$, $2\nu_4(E)$, and $\nu_2 + \nu_4$ bands, respectively. In this case, the upper J and K values for the upper energies were 15 and 11, 15 and 14, 15 and 13, 15 and 11, and 13 and 11 for the ν_1, ν_3, $2\nu_4(A_1)$, $2\nu_4(E)$, and $\nu_2 + \nu_4$ bands, respectively. Strongly speaking, considerably larger transitions

with higher values of quantum numbers J and K were assigned in all studied bands. However, we kept in the final results of the analysis only transitions (and, as a consequence, upper energies) which were assigned without any doubt.

Upper "experimental" rovibrational energies which were derived on the base of assigned transitions for all studied vibrational bands are presented in columns 2, 4, and 6 of Tables 2 and 3 together with their experimental uncertainties Δ (see columns 3, 5, and 7 of Tables 2 and 3). These "experimental" energies and their uncertainties were determined from some transitions reaching the same upper state and are given in Tables 2 and 3 in unity of "cm^{-1}" and "10^{-4} cm^{-1}," respectively.

TABLE 3

Experimental Rovibrational Term Values for the (1000, A_1) and (0002, A_1) Vibrational States of the PH_3 Molecule (in cm^{-1})^a

		(1000,A_1)		(0002,A_1)					(1000,A_1)		(0002, A_1)	
J K Γ		E	Δ	E	Δ	J	K	Γ	E	Δ	E	Δ
1		2	3	4	5		1		2	3	4	5
0 0 A_1		2321.1207		2226.8342		9	0	A_2	2716.2154	6	2636.8998	9
1 0 A_2		2329.9348	5	2236.1457	4	9	1	E	2715.6472	7	2636.0326	11
1 1 E		2329.4117	5	2235.3985	3	9	2	E	2713.9008	10	2634.1548	9
2 0 A_1		2347.5572	4	2254.7361	18	9	3	A_1	2712.2289	18	2629.7463	9
2 1 E		2347.0352	2	2254.1471	7	9	3	A_2	2712.2251	23	2629.2650	6
2 2 E		2345.4697	12	2251.6731	2	9	4	E	2708.1023	11	2623.4656	9
3 0 A_2		2373.9784	4	2282.6427	15	9	5	E	2703.0218	14	2615.6142	3
3 1 E		2373.4555	22	2282.1133	10	9	6	A_1	2698.9115	7	2605.8554	10
3 2 E		2371.8938	5	2279.6872	7	9	6	A_2	2698.9115	7	2605.8554	10
3 3 A_1		2369.2869	3	2275.6085	5	9	7	E	2691.8552	10	2594.1353	5
3 3 A_2		2369.2869	3	2275.6085	5	9	8	E	2683.7947	3	2580.4158	9
4 0 A_1		2409.1848	22	2319.7550	8	9	9	A_1	2674.6614	4	2564.6480	10
4 1 E		2408.6597	15	2319.1425	25	9	9	A_2	2674.6614	4	2564.6480	10
4 2 E		2407.0790	6	2316.7364	11	10	0	A_1	2803.6491	4	2726.4266	16
4 3 A_1		2404.4959	5	2312.6902	6	10	1	E	2803.0635	8	2725.5510	14
4 3 A_2		2404.4959	5	2312.7093	6	10	2	E	2801.3127	9	2722.9103	12
4 4 E		2400.8597	7	2306.9882	2	10	3	A_1	2799.9982	41	2719.0448	7
5 0 A_2		2453.1540	7	2365.7553	10	10	3	A_2	2799.9982	41	2719.6335	2
5 1 E		2452.6279	8	2365.0677	6	10	4	E	2795.7311	9	2713.1868	5
5 2 E		2451.0081	7	2362.6485	4	10	5	E	2790.6020	14	2705.4417	3
5 3 A_1		2448.4967	18	2358.6033	7	10	6	A_1	2786.9550	10	2695.8915	11
5 3 A_2		2448.4967	18	2358.5429	5	10	6	A_2	2786.9550	10	2695.8915	11
5 4 E		2444.7954	8	2352.7285	4	10	7	E	2779.8991	7	2684.4842	4
5 5 E		2440.1792	4	2344.7443	7	10	8	E	2771.8422	11	2671.1811	1
6 0 A_1		2505.8670	13	2420.4947	3	10	9	A_1	2762.7280	6	2655.9365	4
6 1 E		2505.3340	24	2419.7901	7	10	9	A_2	2762.7280	6	2655.9365	4
6 2 E		2503.6724	6	2417.3219	2	10	10	E	2752.4992	16	2638.6738	5
6 3 A_1		2501.2807	7	2413.1047	8	11	0	A_2	2899.7324	9	2824.6510	5
6 3 A_2		2501.2807	7	2413.2350	6	11	1	E	2899.0897	6	2823.7969	11
6 4 E		2497.5045	16	2407.1895	8	11	2	E	2897.3454	9	2821.2619	13
6 5 E		2493.3452	12	2399.1053	4	11	3	A_1	2896.4542	18	2816.9820	10
6 6 A_1		2487.2348	11	2395.0277	11	11	3	A_2	2896.4477	21	2816.3329	12
6 6 A_2		2487.2348	11	2395.0277	11	11	4	E	2892.0479	12	2811.8128	6
7 0 A_2		2567.3004	6	2483.9350	22	11	5	E	2886.8475	8	2804.0620	6
7 1 E		2566.7563	16	2481.9143	6	11	6	A_1	2883.7084	13	2794.6840	14
7 2 E		2565.0567	5	2480.7199	6	11	6	A_2	2883.7084	13	2794.6840	14
7 3 A_1		2562.8418	17	2476.6195	5	11	7	E	2876.6626	10	2783.5467	8
7 3 A_2		2562.8418	17	2476.3939	3	11	8	E	2868.6133	32	2770.6070	6
7 4 E		2558.9709	9	2470.4604	4	11	9	A_1	2859.5198	14	2755.8056	8
7 5 E		2553.9625	19	2462.4071	4	11	9	A_2	2859.5198	14	2755.8056	8
7 6 A_1		2549.0304	4	2452.1561	6	11	10	E	2849.3370		2739.0953	9
7 6 A_2		2549.0304	4	2452.1561	6	11	11	E	2837.9358		2720.3701	9
7 7 E		2542.0096	4	2439.6076	6	12	0	A_1	3004.0749	9	2931.6183	3
8 0 A_1		2637.4247	4	2556.0695	11	12	1	E	3003.6994	10	2930.7076	12
8 1 E		2636.8703	4	2555.1371	14	12	2	E	3001.9720	10	2928.2351	6
8 2 E		2635.1407	8	2552.8868	3	12	3	A_1	2999.0313	19	2923.4892	5
8 3 A_1		2633.1651	12	2548.4370	3	12	3	A_2	2999.0427	21	2924.4745	12
8 3 A_2		2633.1666	18	2548.7812	5	12	4	E	2997.0508	9	2920.3712	11
8 4 E		2629.1770	10	2542.5553	4	12	5	E	2991.7473	13	2911.5636	8
8 5 E		2624.1324	3	2534.5920	6	12	6	A_1	2989.1579	8	2902.2241	6
8 6 A_1		2619.5962	4	2524.6008	10	12	6	A_2	2989.1579	8	2902.2345	2
8 6 A_2		2619.5962	4	2524.6008	10	12	7	E	2982.1353	16		
8 7 E		2612.5523	46	2512.5127	9	12	8	E	2974.0986	19		
8 8 E		2604.4925	20	2498.2946	4	12	9	A_1	2964.8460	12	2864.2676	2

^{a} See footnote to Table 2.

TABLE 3—*Continued*

J K Γ	(1000,A₁) E	Δ	(0002,A₁) E	Δ	J K Γ	(1000,A₁) E	Δ	(0002, A₁) E	Δ
1	2	3	4	5	1	2	3	4	5
12 9 A₂	2964.8460	12	2864.2676	2	14 0 A₁	3238.9728	7		
12 10 E	2954.8002	19	2848.0332	11	14 1 E	3238.5859	31		
12 11 E	2945.1822	2			14 2 E	3236.9327	22		
13 0 A₂	3117.2900	12	3047.0252	9	14 3 A₁	3234.5789	17		
13 1 E	3116.8708	10	3046.2749	11	14 3 A₂	3234.3552	16		
13 2 E	3115.1665	13	3043.8553	6	14 6 A₁			3144.7425	19
13 3 A₁	3112.3627	22	3040.3299	19	14 6 A₂	3226.3835	18	3144.7573	
13 3 A₂	3112.3542	18			14 7 E	3219.4752	9		
13 4 E	3108.4906	12			14 8 E	3211.4523	11	3156.9007	8
13 5 E	3105.3631	8			14 9 A₁			3141.0821	10
13 6 A₁	3103.3349	10	3018.6368	8	14 9 A₂			3141.0821	10
13 6 A₂	3103.3349	10	3018.6219	3	14 10 E			3127.6135	
13 7 E	3096.3303	7			14 12 A₁			3092.8080	4
13 8 E	3088.2895	6			14 12 A₂			3092.8080	4
13 9 A₁	3079.1931	13	2981.2925	13	14 13 E			3071.9668	8
13 9 A₂	3079.1931	13	2981.2925	13	15 0 A₂	3369.4688	10		
13 10 E	3069.0303	10			15 13 E			3212.0411	10

The Δ is not quoted when the upper energy value was obtained from only one transition.

Assignments of transitions and analysis of the obtained data showed the presence of numerous different a₁–a₂ splittings. In this case, the experimental recorded spectrum allowed us to see the a₁–a₂ splittings not only for the rovibrational states with the value of quantum number K equals to 3 for the bands ν₁ and 2ν₄(A₁), or K = 1 and/or 2 for the bands ν₃, 2ν₄(E), and ν₂ + ν₄, but for states with the value of quantum number K equals to 4, 5, 6, and even 7, 8, and 10, as well. Some examples of such high K-value doublets are shown in Figs. 6 and 7. In Fig. 6 the experimentally observed ᴾQ₆ₐ₁/ₐ₂(J) doublets in the 2ν₄(E) band are presented. The P-branch's a₁–a₂ doublets in the ν₂ + ν₄ and ν₃ bands, which correspond to the upper states with K = 7 and 8, respectively, are shown

in Fig. 7. In this case, one of the appearances of strong resonance interaction can be seen in Fig. 7. Namely, in ordinary situations, the value (−1)ᴶ(E[JK a₁] − E[JK a₂]) has the same sign for any value of quantum number J. At the same time, as one can see from the lower part of Fig. 7, the components of the ᴾP₉ₐ(15) doublet of the ν₃ band are inverted with respect to the components of the corresponding ᴾP₉ₐ(13) doublet.

The collected information concerning the observed and analyzed a₁–a₂ doublets is presented in Tables 4 and 5. In this case, Table 4 gives the list of minimum values of the quantum number J which correspond to the first appearances of

TABLE 4

Minimum Values of Quantum Number J Which Correspond to the First Appearance of the a₁ and a₂ Splittings in the Sets of States [JKaλ]

Value of K	(1000, A₁)	(0010, E)	(0002, A₁)	(0002, E)	(0101, E)
1		1		1	1
2		2		2	4
3	8		4		
4		10		10	6
5		11		6	
6			12		
7		14			10
8		12		9	
10		14			

TABLE 5

Values of the a₁ and a₂ Splittings for Rovibrational States [J = 12 K] Derived from the Experimental Spectrum of the PH₃ Molecule (in cm⁻¹)

Value of K	(1000, A₁)	(0010, E)	(0002, A₁)	(0002, E)	(0101, E)
1		1.3020		0.3628	17.0598
2		1.8945		18.6575	0.3798
3	0.0114		0.9653		
4		0.1850		0.1437	1.2981
5		0.0072		1.8805	
6			0.0104		
7		0.0606ᵃ			0.0583
8		0.0447	0.6096ᵇ		
10		0.0665ᵃ			

ᵃ The value of splitting corresponds to the [J = 14 K] states because the first splittings of the states with K = 7 and 10 were observed for the states [J = 14 K].
ᵇ The value of splitting corresponds to the [J = 11 K = 8] states because transitions with the upper states [J = 12 K = 8, aλ] have not been assigned in the spectrum.
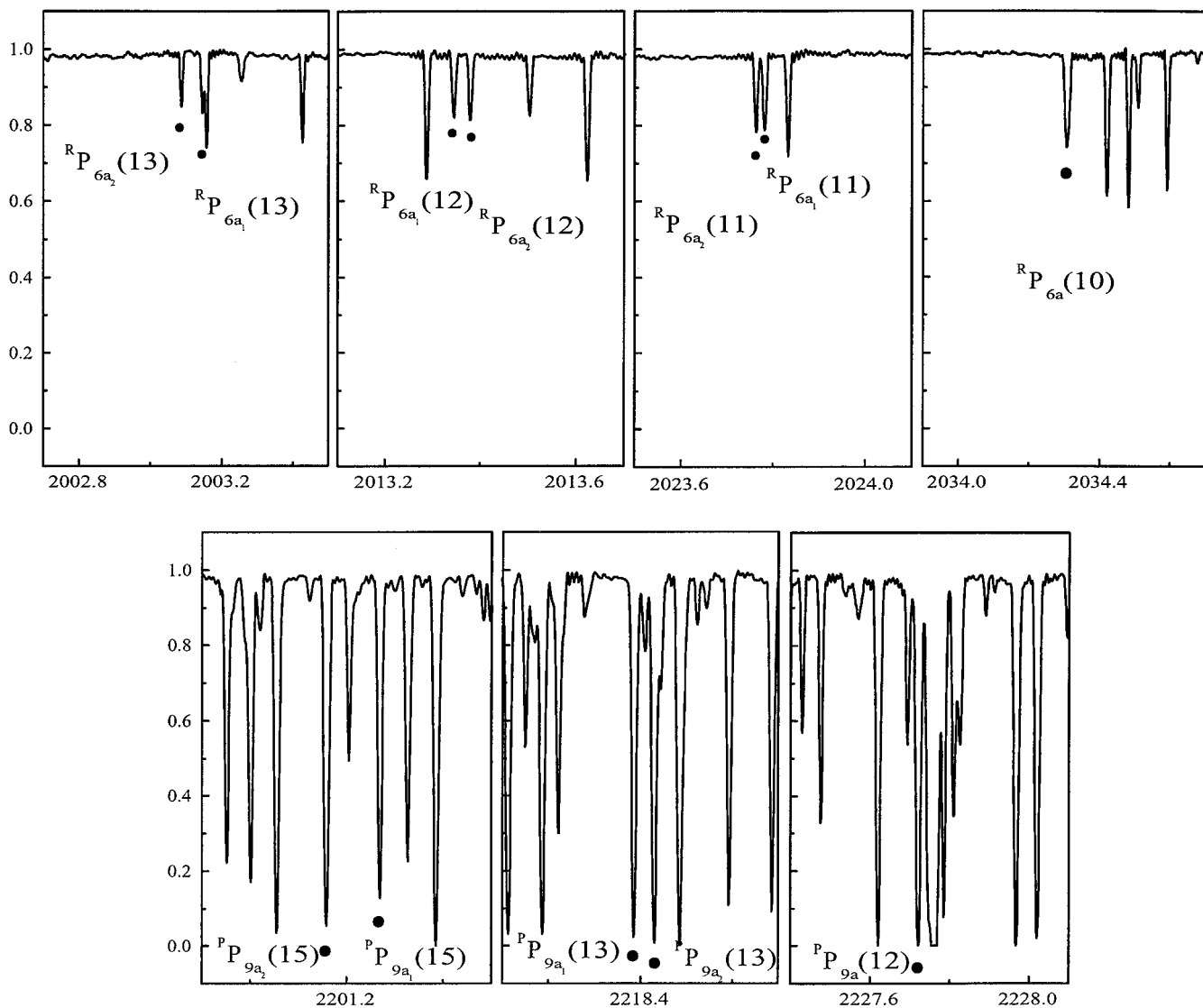
FIG. 7. Two sets of P-branch transitions leading to the split of the $[J^{upper} K^{upper} = 7a_1/a_2]$ states of the $\nu_2 + \nu_4$ band (upper part) and of the $[J^{upper} K^{upper} = 8a_1/a_2]$ states of the ν_3 band (upper part). The inversion of components of the $[a_1 - a_2]$ doublets can be seen from comparison of the $^P P_{9a}(13)$ and $^P P_{9a}(15)$ transitions at the bottom of the figure.

the $a_1 - a_2$ splittings in the sets of states $[JK\Gamma](v_1 v_2 v_3 v_4)$ with different values of the quantum number J and fixed values of other quantum numbers. To give the reader a notion of the comparative values of $a_1 - a_2$ splittings, Table 5 presents such splittings for the rovibrational states $[J = 12 K\ a_1/a_2](v_1 v_2 v_3 v_4)$ of all five studied vibrational states. In this case, because splittings begin with the value of $J = 14$ for the states with $K = 7$ and 10 for the vibrational state $(0010, E)$, corresponding values in Table 5 are presented not for the value of $J = 12$, but for $J = 14$. All values in Table 5 are given in cm^{-1}.

The largest splittings are seen for the set of states $[JK = 2a_1/a_2](0002, E)$. As the analysis shows, the reason for these

splittings lies in the presence of a strong resonance interaction of the $(J_+^2 \pm J_-^2)$ type between the vibrational states $(0002, E)$ and $(0002, A_1)$. In turn, the presence of these large splittings leads to the appearance of anomalously large $a_1 - a_2$ splittings for the states $[JK = 5a_1/a_2]$ and $[JK = 8a_1/a_2]$ of the $(0002, E)$ vibrational state. The same deduction can be made with respect to the $a_1 - a_2$ splittings for the states $[JK = 4a_1/a_2]$ and $[JK = 7a_1/a_2]$ of the $(0101, E)$ vibrational state. In this case, the presence of giant splittings corresponding to the states with $K = 1$ is the reason for the appearance of $K = 4$ and $K = 7$ splittings.

The presence of numerous resonance interactions can lead, not only to anomalously large splittings for lower values of

TABLE 6
Energy Values of Some Rovibrational States of the a_1 and a_2 Symmetry[a]

J	$E_{[JK=1a_1]}$	$E_{[JK=1a_2]}$	Δ[b]	$E_{[JK=0a_\lambda]}$	$E_{[JK=2a_1]}$	$E_{[JK=2a_2]}$
	(0002, E)	(0002, E)	(0002, E)	(0002, A$_1$)	(0002, E)	(0002, E)
1	2	3	4	5	6	7
1	2236.3808	2236.4531	0.0723	2236.1457		
2	2255.1932	2255.0020	0.1912	2254.7361		2273.8205
3	2283.0536	2283.2551	0.2015	2282.6427	2301.7070	2301.9262
4	2320.7193	2320.6458	0.0735	2319.7550	2339.4814	2338.8479
5	2367.8285	2367.8078	−0.0207	2365.7553	2385.2054	2386.5930
6	2424.4457	2424.4842	−0.0385	2420.4947	2443.2608	2440.7311
7	2490.4292	2490.4214	−0.0078	2483.9350	2505.3686	2509.3782
8	2565.5303	2565.4768	0.0535	2556.0695	2584.7014	2579.0616
9	2649.4678	2649.6056	0.1378	2636.8998	2661.7618	2671.3992
10	2742.5081	2742.2555	0.2526	2726.4266	2765.6520	2753.4658
11	2843.7712	2844.1291	0.3579	2824.6510	2854.52[c]	2869.1139
12	2954.3885	2954.0257	0.3628	2931.6183	2981.5174	2962.8599
13	3072.8882	3073.2689	0.3807	3047.0252	3081.02[c]	3103.0021

[a] All the values are given in cm^{-1}.
[b] Here Δ is the difference $(-1)^J (E_{[JK=1a_1]} - E_{[JK=1a_2]})$.
[c] Estimated from calculations.

quantum number K and to the appearance of exotic splittings for the states with higher values of K, but to anomalous behavior and even inversions of relative positions of the a_1 and a_2 components of doublets in some series of energy levels. One such situation was mentioned above (see the lower part of Fig. 7). As one more interesting example, the set of the states $[JK = 1a_1/a_2](0002, E)$ can be mentioned. For an illustration of the situation, Table 6 presents corresponding pairs of energy levels $E_{JK=1a_1}$ and $E_{JK=1a_2}$. One can see that the splittings begin already with the value of quantum number $J = 1$. The value of the splitting is first increased. But, already from the value of J equal to 4, it begins to decrease, and for the value $J = 5$ it even changes sign. Between values of J equal to 7 and 8, the relative position of the energy levels is inverted again. Then the value of the split begins to increase rapidly, but near the value $J = 11$ the increase is stopped, and up to the value $J = 13$ the value of the split is practically not changed. The reasons for such more than unusual behavior are the following: at the first step, two different interactions have an effect on the value of the a_1–a_2 splitting of the states $[JK = 1a_1](0002, E)$ and $[JK = 1a_2](0002, E)$. The first is caused by the operators $C(J_+^2 \pm J_-^2)$ (see Eqs. [6], [7]), which provide the ordinary a_1–a_2 splitting of the states $[JK = 1a_1]$ and $[JK = 1a_2]$. The second is the operators of type $A^*(J_+ \pm J_-)$ (see Eq. [13]), which provide the strong resonance interaction between the states $[JK = 1a_\lambda](0002, E)$ and $[JK = 0a_\lambda](0002, A_1)$. Moreover, as the analysis shows, these have opposite effects on the shifts of the energy levels $E_{[JK=1a_1]}$ and $E_{[JK=1a_2]}$. In this case, as one can see from columns 2, 3, and 5 of Table 6, the distance

between the levels $[JK = 0a_\lambda](0002, A_1)$ and the corresponding levels $[JK = 1a_\lambda](0002, E)$ increases with the increasing value of quantum number J. As a consequence, the efficiency of the $A^*(J_+ \pm J_-)$ resonance interaction is quickly decreased (see the behavior of the curve I in Fig. 8 up to the value $J = 6$). In this case, the relative positions of the a_1 and a_2 components are even inverted. At the same time, starting from the value of the quantum number $J = 6$, the third mechanism of interaction begins to be more and more important. It is the $A(J_+ \pm J_-)$ operators (see Eqs. [6], [7]), which provide, in particular, interactions between the states $[JK = 1a_\lambda]$ and $[JK = 2a_\lambda]$ of the vibrational state (0002, E) (see columns 6 and 7 of Table 6). In this case, beginning from the value of $J = 7$, the value of the split decreases again (see column 3 of Table 6 and Fig. 8) and, for the second time, the a_1 and a_2 components are inverted. Finally, the joint influence of all three mechanisms leads to the practically unchanged value of the splittings for the values of the quantum number $J = 11$–13. For comparison with the exotic behavior of the discussed splittings, the curve II in Fig. 8 illustrates the ordinary dependence of the splitting on the value of the quantum number J.

As was mentioned above, assignments of transitions (especially the states with $J^{upper} > 10$) were made simultaneously with a fit of upper energies. In this case, theoretical estimates with the parameters derived from the fit allowed us to predict wavenumbers of new unassigned transitions with more than satisfactory accuracy (about 0.01–0.03 cm^{-1}, as a rule). Finally, we were able to reproduce 1008 derived upper levels ($J \leq 15$) with an *rms* deviation of 0.0039 cm^{-1}. However, the total of 157 parameters of the Hamiltonian obtained from the fit seems to be extremely large. On this reason we present
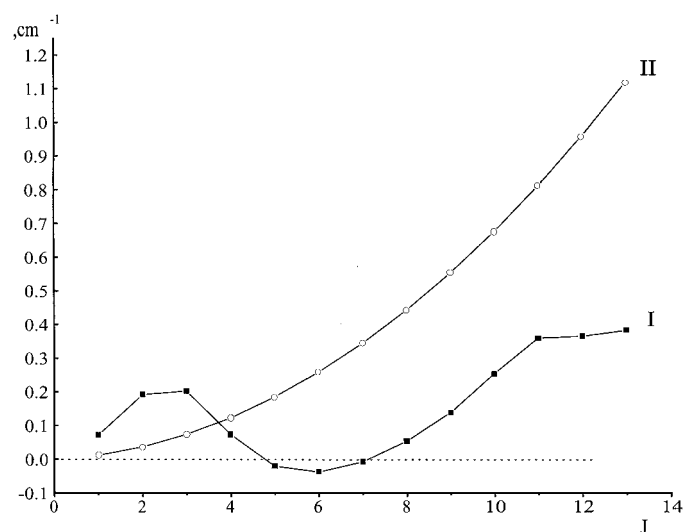
FIG. 8. Illustration of the anomalous dependence of the "experimental" a_1–a_2 splittings on the value of the quantum number J for the states $[JK = 1a_1/a_2](0002, E)$ (curve I; see text for details). For comparison, the corresponding normal dependence is indicated by curve II.

here only the results of assignments and do not present these parameters.

5. CONCLUSION

The infrared spectrum of the phosphine, PH_3, has been recorded in the region of the bands ν_1, ν_3, $\nu_2 + \nu_4$, and $2\nu_4$, and transitions belonging to these bands were assigned up to the value of quantum number J^{upper} 15, 15, 13, and 15, respectively. Numerous $a_1 - a_2$ splittings in the recorded spectrum were observed and theoretically described for the values of quantum number K $1 \leq (K \neq 9) \leq 10$.

ACKNOWLEDGMENTS

REFERENCES

1. A. T. Tokunaga, R. F. Knacke, S. T. Ridgway, and L. Wallace, *Astrophys. J.* **232,** 603–615 (1979).
2. R. F. Knacke, S. J. Kim, S. T. Ridgway, and A. T. Tokunaga, *Astrophys. J.* **262,** 388–395 (1982).
3. L.-M. Lara, B. Bezard, C. A. Griffith, J. H. Lacy, and T. Owen, *Icarus* **131,** 317–333 (1988).
4. P. Drossart, E. Lellouch, B. Bezard, J.-P. Maillard, and G. Tarrago, *Icarus* **83,** 248–253 (1990).
5. K. S. Noll and H. P. Larson, *Icarus* **89,** 168–189 (1990).
6. O. N. Ulenikov, O. L. Petrunina, E. S. Bekhtereva, E. A. Sinitsin, H. Bürger, and W. Jerzembeck, *J. Mol. Spectrosc.*, in press (2002).
7. O. N. Ulenikov, E. S. Bekhtereva, O. L. Petrunina, H. Bürger, and W. Jerzembeck, submitted for publication.
8. A. Ainetschian, U. Häring, G. Spiegl, and W. A. Kreiner, *J. Mol. Spectrosc.* **181,** 99–107 (1996).
9. D. C. McKean and P. N. Schatz, *J. Chem. Phys.* **24,** 316–325 (1956).
10. A. Baldacci, V. Malathy Devi, K. Narahari Rao, and G. Tarrago, *J. Mol. Spectrosc.* **81,** 179–206 (1980).
11. G. Tarrago, N. Lacome, A. Levy, G. Guelachvili, B. Bezard, and P. Drossart, *J. Mol. Spectrosc.* **154,** 30–42 (1992).
12. O. N. Ulenikov, A. B. Malikova, S. Alanko, M. Koivusaari, and R. Anttila, *J. Mol. Spectrosc.* **179,** 175–194 (1996).